PNAS RESEARCH ARTICLE | PLANT BIOLOGY

DMP8 and 9 regulate HAP2/GCS1 trafficking for the timely acquisition of sperm fusion competence

Wei Wang[a,1], Hanxian Xiong[b,1], Peng Zhao[a], Xiongbo Peng[a], and Meng-Xiang Sun[a,2]

Edited by June Nasrallah, Cornell University, Ithaca, NY; received May 7, 2022; accepted October 11, 2022

Sexual reproduction involves the fusion of two gametes of opposite sex. Although the sperm-expressed fusogen HAPLESS 2 (HAP2) or GENERATIVE CELL SPECIFIC 1 (GCS1) plays a vital role in this process in many eukaryotic organisms and an understanding of its regulation is emerging in unicellular systems [J. Zhang *et al.*, *Nat. Commun.* 12, 4380 (2021); J. F. Pinello *et al. Dev. Cell* 56, 3380–3392.e9 (2021)], neither HAP2/GCS1 interactors nor mechanisms for delivery and activation at the fusion site are known in multicellular plants. Here, we show that *Arabidopsis thaliana* HAP2/GCS1 interacts with two sperm DUF679 membrane proteins (DMP8 and DMP9), which are required for the EGG CELL 1 (EC1)-induced translocation of HAP2/GCS1 from internal storage vesicle to the sperm plasma membrane to ensure successful fertilization. Our studies in *Arabidopsis* and tobacco provide evidence for a conserved function of DMP8/9-like proteins as HAP2/GCS1 partner in seed plants. Our data suggest that seed plants evolved a DMP8/9-dependent fusogen translocation process to achieve timely acquisition of sperm fusion competence in response to egg cell–derived signals, revealing a previously unknown critical step for successful fertilization.

sperm cell | gamete fusion | regulated exocytosis | HAP2 | DMP8/9

Significance

During sexual reproduction, gamete fusion is delicately mediated by cell-surface proteins to ensure successful fertilization. In eukaryotes, the only gamete fusogen identified so far is HAP2/GCS1. Although information about HAP2/GCS1 regulation is emerging in unicellular alga, nothing is known about regulation or protein interactors of this fusion-essential protein in multicellular plants. Here, we reveal that two sperm-expressed DUF679 membrane proteins (DMP8/9) directly interact with HAP2/GCS1 and colocalize with HAP2/GCS1 on discrete cytoplasmic organelles. DMP8/9 responds to egg cell signal EC1 and translocates HAP2/GCS1 to the sperm plasma membrane for egg–sperm fusion. Furthermore, our work suggests that this mechanism underlying sperm cell activation is conserved in seed plants.

Fertilization depends on the fusion of two haploid gametes of opposite sex. Like other cell–cell fusion events, adhesion proteins bring the opposing plasma membranes (PMs) into close proximity, whereas membrane merger is mediated by fusogens (1, 2). Although several fertilization-essential proteins have been identified in multiple model organisms, gamete fusogens have not yet been identified in fungi and chordates (3–6). On the other hand, the conserved membrane protein HAPLESS 2 (HAP2), which is also called GENERATIVE CELL SPECIFIC 1 (GCS1), is essential for gamete fusion in many unicellular organisms, in several animal taxa, and in higher plants (7–15). Remarkably, HAP2/GCS1 shares structural similarity with viral class II fusion proteins (16–18). These viral proteins are on the virus surface as homo- or heterooligomers and undergo a low pH-triggered fusogenic reconfiguration upon endocytosis into target cells (19–21). Recent studies indicate that, as in class II fusion protein-dependent viral fusion, gamete membrane fusion in HAP2/GCS1-expressing organisms also depends on reconfiguration of this eukaryotic class II fusion protein into stable homotrimers (22). In contrast to the viral proteins, however, the fusogenic reconfiguration of HAP2/GCS1, at least in the unicellular green alga *Chlamydomonas reinhardtii*, is not regulated by pH but depends on HAP2/GCS1 *cis* interactions with a species-specific membrane adhesion protein, MAR1 (23). HAP2/GCS1 reconfiguration is initiated during gamete adhesion, when MAR1 binds to the *Chlamydomonas* member of the sperm adhesion protein family, FUS1/GAMETE EXPRESSED 2 (GEX2) (23–26). In mammals and several other animal groups for which fertilization-related proteins are known, many are stored intracellularly, often on the membrane of a specialized secretory vesicle, the acrosome, and an exocytic event, the acrosome reaction, is required to relocate them at the right time to the site of sperm–oolemma binding and fusion (27–32). Although plant sperm lack an acrosomal vesicle per se, HAP2/GCS1 in *Arabidopsis thaliana* is stored on endomembranes, and regulated exocytosis is required for its delivery to the PM during the process of double fertilization (33). Thus, when they first arrive in the vicinity of the egg, *Arabidopsis* sperm are not competent for adhesion and fusion, and then they become activated by egg cell–secreted, small, cysteine-rich proteins called EGG CELL 1 (EC1) proteins. In in vitro studies, synthetic EC1 peptides induce the translocation of the HAP2/GCS1 from endomembrane compartments to the sperm cell surface (33–35). To date, the HAP2/GCS1 protein interactors required for this regulated delivery of HAP2/GCS1 to the cell surface remain unknown.

Fertilization in flowering plants such as *Arabidopsis* is unique as it involves two sets of reproductive cells (egg and central cell). In a process termed double fertilization, two

Author affiliations: [a]State Key Laboratory of Hybrid Rice, College of Life Sciences, Wuhan University, Wuhan 430072, China; and [b]School of Life Science and Technology, Wuhan Polytechnic University, Wuhan 430023, China

Author contributions: M.X.S. designed research; W.W. and H.X. performed research; M.X.S. contributed new reagents/analytic tools; H.X., P.Z., X.P., and M.X.S. analyzed data; and W.W. and M.X.S. wrote the paper.

The authors declare no competing interest.

This article is a PNAS Direct Submission.

[1]W.W. and H.X. contributed equally to this work.

[2]To whom correspondence may be addressed. Email: mxsun@whu.edu.cn.

This article contains supporting information online at http://www.pnas.org/lookup/suppl/doi:10.1073/pnas.2207608119/-/DCSupplemental.

Published November 2, 2022.

nonmotile and interconnected sperm cells are delivered into the ovule by a pollen tube and coordinately fertilize two female reproductive cells, giving rise to a diploid embryo and a triploid endosperm (6, 36). Beside the fusogen HAP2/GCS1, two other types of membrane proteins with key roles in gamete adhesion and fusion have been discovered in *Arabidopsis* sperm cells. The *Arabidposis* FUS1/GEX2 family, GEX2, serves as adhesion factor (26), whereas two small integral DUF679 membrane proteins (DMPs) with four predicted transmembrane domains (TMDs), namely DMP8 and DMP9, redundantly support gamete fusion (35, 37, 38). It was reported that the fertilization rate was reduced over twofold in *Arabidopsis dmp8/9* mutants and *dmp8/9* sperm cells could adhere to the egg cell but fail to fuse (35, 37), indicating that DMP8 and 9 function at the fusion step of fertilization by a yet-unknown molecular mechanism.

Here, we uncover molecular functions of the DMP8/9 proteins. We show that DMP8/9 bind to HAP2/GCS1 within sperm. Moreover, we find that DMP8/9 are essential for the EC1-induced translocation of HAP2/GCS1 from discrete vesicle-like structures within sperm to the sperm PM where the proteins remain associated. Two sets of findings indicate that DMP8/9 function is broadly conserved across seed plants. Disruption of genes for the equivalent DMP proteins in *Nicotiana* disrupts seed set, and DMP8/9-like proteins from *Nicotiana* and other angiosperms, including *Amborella trichopoda*, rescue seed set in *Arabidopsis dmp8/9* mutants.

Results

DMP8 and DMP9 Are Required for EC1-Induced Redistribution of HAP2/GCS1 to the Sperm Cell Surface. To investigate whether DMP8 and 9 are involved in EC1-induced sperm activation, we crossed HAP2/GCS1-RFP (red fluorescent protein) (Col-0 background) with *dmp8 dmp9* (*dmp8/9*) double mutants and observed the expression and subcellular localization of HAP2-RFP in *dmp8/9* sperm cells. The *dmp8/9* double mutant, generated by crossing two previously undescribed transfer DNA (T-DNA) insertion lines, showed reduced male fertility and unfused sperm phenotypes comparable to those reported for CRISPR/Cas9 gene-edited double mutants (Fig. 1 *A* and *B* and *SI Appendix*, Figs. S1 and S2) (35, 38, 39). Compared with that in wild type (WT), subcellular location of HAP2/GCS1-RFP is not altered in sperm cells lacking functional *DMP8* and *DMP9,* no matter in pollen grains or in pollen tubes (*SI Appendix*, Fig. S3 *A* and *B*). Next, we tested the ability of *dmp8/9* sperm cells carrying HAP2/GCS1-RFP responding to EC1 peptides after they had been released from pollen tubes growing in a semi-in vivo system (Fig. 1*C* and *SI Appendix*, Fig. S3*C*). When treated with control solution lacking EC1 peptides (−EC1pep), no matter in WT or *dmp8/9* sperm, HAP2/GCS1 appeared to be in these large and peripherally distributed particles, whereas when treated with EC1 peptide mixtures HAP2/GCS1 in WT became diffuse and most was evenly distributed at the cell membrane. By contrast, HAP2/GCS1 in *dmp8/9* was still in the large particles, indicating that *dmp8/9* sperm cells failed to respond to EC1 peptides and translocate HAP2/GCS1-RFP from internal membranes to the PM (Fig. 1 *C* and *D* and *SI Appendix*, Fig. S3*C*).

In planta imaging supported the finding that DMP8/9 and EC1 proteins are required for the trafficking of HAP2/GCS1 to the sperm cell surface. In these assays, emasculated flowers were hand-pollinated with HAP2/GCS1-RFP–expressing pollen (Col-0 background) and dissected for microscopy 8 to 9 h later. Since WT sperm cells fuse ∼7.4 min after pollen tube discharge (40), they are hardly ever detected at the site of gamete fusion within the ovule. In those exceptional cases, HAP2/GCS1-RFP was clearly detectable at the cell surface but not in endomembrane compartments of sperm cells within the embryo sacs (Fig. 1*E*), which was different from HAP2/GCS1-RFP distribution within pollen tubes (*SI Appendix*, Fig. S3*B*). When pollen from HAP2/GCS1-RFP–expressing *dmp8/9* mutant plants was used, 79.2% of sperm cells retained HAP2/GCS1-RFP on internal membranes. Likewise, 86.4% of WT sperm cells retained HAP2/GCS1-RFP on internal membranes when they were delivered into *5xec1* ovules lacking the expression of all five *EC1* genes due to CRISPR/Cas9 gene editing of *EC1.2* in a *4xec1* knockout genetic background (Fig. 1*E*).

DMP9 Interacts with HAP2/GCS1 and Colocalizes with HAP2/GCS1 on Organelle-Like Structures in Sperm Cells. Next, we studied the subcellular localization of DMP9 and HAP2/GCS1 in sperm cells released from semi-in vivo growing pollen tubes in transgenic plants coexpressing DMP9-GFP (green fluorescent protein) and HAP2/GCS1-RFP by their own promoters (Col-0 background). Notably, DMP9-GFP was detected at the sperm PM and on up to five discrete organelle-like structures, where it colocalized with HAP2/GCS1-RFP (Fig. 1*F*). A few more spherical but slightly larger internal structures were only positive for HAP2/GCS1-RFP but lacked DMP9-GFP signals. In comparison to sperm cells treated with EC1-free control solution, the application of EC1 peptides significantly induced the formation of PM patches with colocalizing red and green fluorescence (Fig. 1 *F* and *G*). These strong signals at the PM are indicative of the joint exocytic translocation of HAP2/GCS1 and DMP9 from the intracellular organelle-like compartments to the cell surface in response to EC1 peptides. EC1-induced local translocation to the PM was also observed in WT sperm cells solely expressing DMP9-GFP (Fig. 1 *H* and *I*), arguing against a cooverexpression phenotype. We also crossed DMP9-GFP line with +/*hap2* mutants and found that DMP9-GFP expression and localization in +/*hap2* sperm cells were indistinguishable from that in WT sperm (*SI Appendix*, Fig. S4*B*). Moreover, the ability that EC1-induced DMP9 translocation to the PM was not influenced when absence of functional HAP2/GCS1 (*SI Appendix*, Fig. S4 *B* and *C*). Thus, DMP8/9-relevant properties are independent of HAP2/GCS1. Nonetheless, coimmunoprecipitation experiments did not provide evidence for a direct physical interaction between DMP9 and EC1, supporting the conclusion that EC1 acts upstream of DMP8/9 (*SI Appendix*, Fig. S4 *E* and *F*).

The colocalization with HAP2/GCS1 and the necessity of DMP8/9 for EC1-induced HAP2/GCS1 trafficking to the sperm cell surface prompted us to test their direct interactions in membrane-based yeast two-hybrid (MbY2H) and pull-down assays (using maltose binding protein [MBP]-tagged HAP2/GCS1$_{ecd}$, 25–530, and intein-tagged DMP8/9). Notably, both assays revealed physical interactions between HAP2/GCS1 and DMP8 or DMP9, respectively (Fig. 2 *A*–*C* and *SI Appendix*, Fig. S5). Their role as HAP2/GCS1 partner proteins was further supported *in planta* by coimmunoprecipitation of the FLAG-tagged HAP2/GCS1$_{ecd}$ with HA-tagged DMP8 and DMP9 (Fig. 2*D* and *SI Appendix*, Figs. S4*D* and S5 *D* and *E*).

DMP3^{DMP9N} Can Replace DMP8 and DMP9 as HAP2/GCS1 Partner Protein. Ten *DMPs* are present in the genome of *Arabidopsis*, with four gene pairs encoding rather similar proteins (DMP1/2, DMP3/5, DMP4/6, and DMP8/9), most likely a result of gene duplications (41). Functional redundancies among *Arabidopsis*

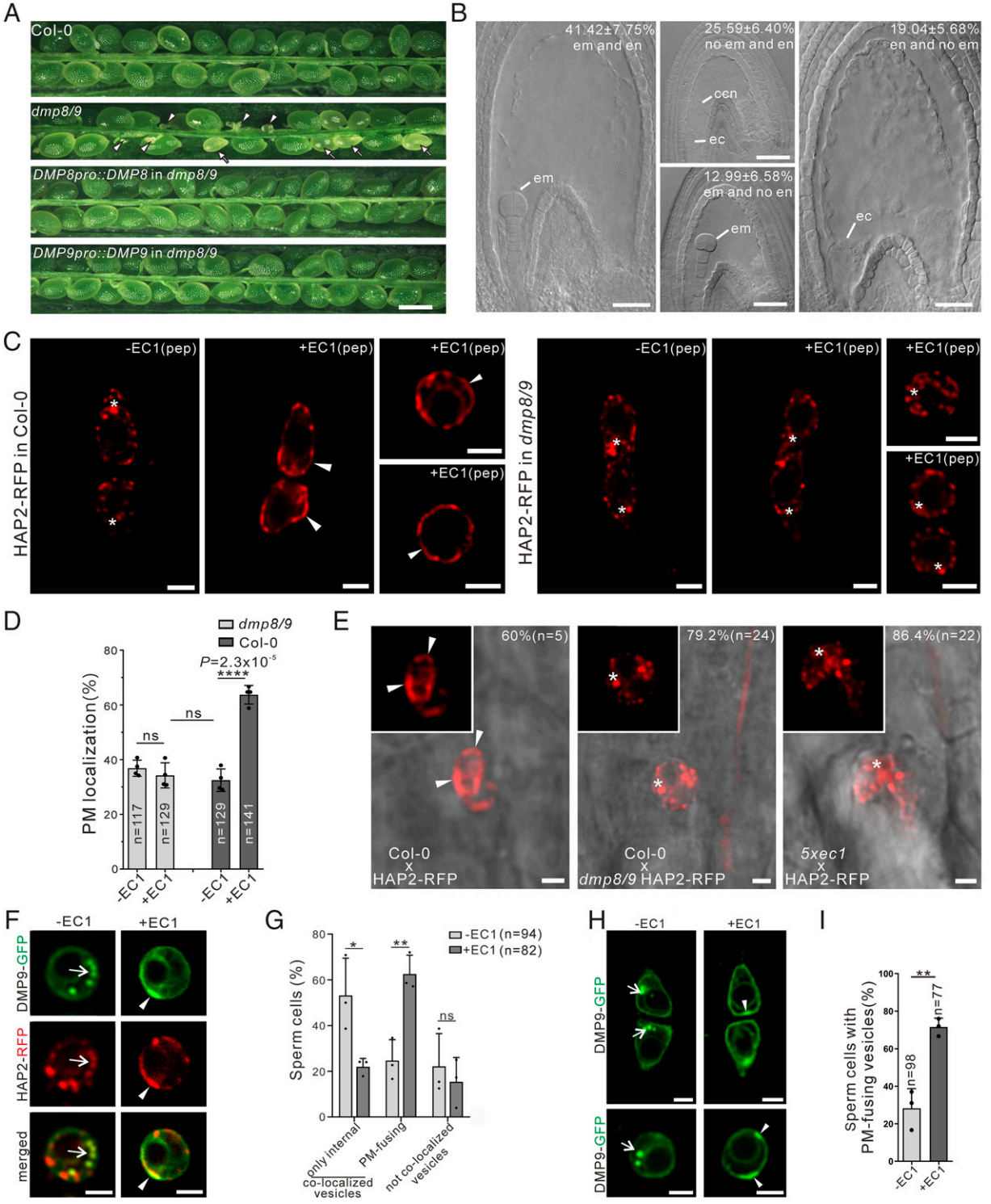

Fig. 1. *Arabidopsis* DMP8 and DMP9 are required for the EC1-triggered accumulation of HAP2/GCS1 at the sperm-cell surface. (*A*) Aborted seeds (arrows) and unfertilized ovules (arrowheads) were frequently detected in siliques harvested from the *dmp8/9* double mutants. Seed set was restored when *dmp8/9* was complemented either with *DMP8* or *DMP9*. (Scale bars, 1 mm.) (*B*) Cleared *dmp8/9* ovules, 3 d after pollination. ccn, central cell nuclei; ec, egg cell; em, embryo; en, endosperm. Frequency of phenotype (mean ± SD) is shown on the top right with 0.96 ± 1.93% unidentified seeds (n = 526). (Scale bars, 20 μm.) (*C*) In *dmp8/9* sperm cells the EC1 peptide mix (+EC1pep) has no stimulating effect on the redistribution of HAP2/GCS1-RFP from internal membranes (asterisks) to the PM (arrowheads). HAP2/GCS1-RFP in the Col-0 background (WT) and peptide-free solution (-EC1pep) served as controls. (Scale bars, 2 μm.) (*D*) Quantification of sperm cells with HAP2/GCS1-RFP at the PM. Mean values ± SD of four independent experiments are shown. (*E*) HAP2/GCS1-RFP–expressing sperm cells at the fusion site of ovules, 8 to 9 h after pollination, imaged by confocal laser scanning microscopy (CLSM). HAP2/GCS1-RFP signals on the sperm PM (arrowheads) and on internal membranes (asterisks). (Scale bars, 2 μm.) (*F*) WT sperm cells coexpressing DMP9-GFP and HAP2/GCS1-RFP. HAP2/GCS1-RFP colocalized with DMP9-GFP in intracellular vesicle-like bodies (arrows, -EC1) and at PM areas (arrowheads, +EC1). CLSM single optical sections are shown. (Scale bar, 2 μm.) (*G*) Quantification of DMP9 and HAP2/GCS1 colocalization. (*H*) DMP9-GFP signals in Col-0 sperm cells released from the pollen tubes. Within the cytoplasm of a sperm cell, up to six spherical structures with green fluorescence (arrows) are visible, suggesting that DMP9-GFP localizes to organelles of the secretory pathway. When the sperm cells are treated with the EC1 peptide mix (+EC1), the DMP9-GFP fluorescent organelle-like structures fuse with the PM (arrowheads). Peptide-free solution (-EC1) was used as a reference. (Scale bars, 2 μm.) (*I*) Quantification of sperm cells with PM-fusing organelle-like structures, showing a significant difference between sperm cells treated with peptide-free control solution (25.7%) and those treated with EC1 peptides (71.6%). Data are the means ± SD. Significant differences (two-sided Student's *t* test): ns, not significant; *P < 0.05; **P < 0.01; ****P < 0.0001.

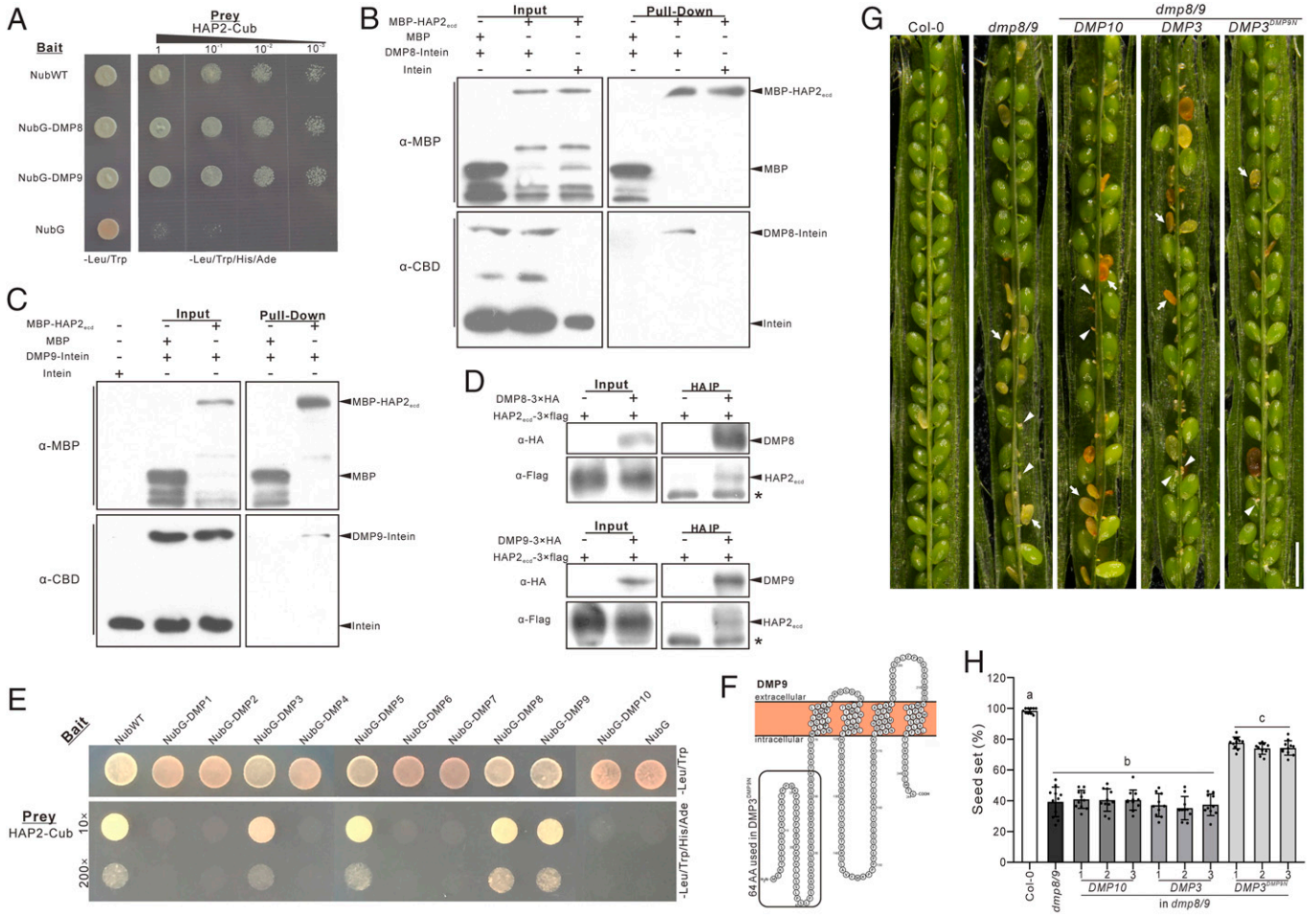

Fig. 2. DMP8 and DMP9 interact with HAP2/GCS1 and their function in HAP2/GCS1-mediated gamete fusion is not restored by *DMP10* but by *DMP3*^{DMP9N}. (*A*) HAP2/GCS1 interacts with DMP8 and DMP9 in a membrane-based yeast-two-hybrid (MbY2H) system. (*B* and *C*) Pull-down assays showing that the recombinant MBP-tagged extracellular domain of HAP2/GCS1(MBP-HAP2/GCS1$_{ecd}$, 25–530) interacts with the recombinant intein-tagged DMP8 and DMP9. MBP-HAP2/GCS1$_{ecd}$ and MBP protein in bacterial lysates were bound to amylose resin followed by incubation of those beads with the intein-tagged DMP8 or DMP9 crude protein extracts. (*D*) Co-IP assays prove in vivo interactions. HAP2/GCS1$_{ecd}$-3xFLAG (59 kDa) and 3xHA-tagged DMP8 or DMP9 (31 kDa) were coexpressed in *N. benthamiana* leaf cells, followed by immunoprecipitation using anti-HA agarose. Asterisks indicate the heavy chain of the IgG used for HA IP (~ 50 kDa). (*E*) HAP2/GCS1 in MbY2H assays with all 10 *Arabidopsis* DMPs reveals additional interaction with DMP3 and DMP5. NubG, as negative control; NubWT, as positive control. Note that the yeast strain cotransformed with HAP2/GCS1 and four DMPs (DMP3, 5, 8, 9) can grow on selective SD medium (-Leu-Trp-His-Ade). (*F*) A scheme depicting the predicted DMP9 transmembrane topology and the DMP9-N terminus region used in DMP3^{DMP9N}. The scheme was prepared by Protter (wlab.ethz.ch/protter/start/) using transmembrane regions annotated by UniProt and the N-terminal location intracellular. (*G* and *H*) Reduced seed set in *dmp8/9* is not restored by sperm-expressed *DMP10*, *DMP3* but by *DMP3*^{DMP9N}. (*G*) Siliques from Col-0 (WT), *dmp8/9*, and *dmp8/9* expressing either *DMP9p:DMP10*, *DMP9p:DMP3*, or *DMP9p:DMP3*^{DMP9N}. (Scale bar, 1 mm.) (*H*) Quantification of seed set for Col-0, *dmp8/9*, and three independent transgenic lines each for *dmp8/9* complemented either with *DMP10*, *DMP3*, or *DMP3*^{DMP9N}. Siliques from T1 generations are shown. Significant differences ($P < 0.0001$ by two-sided Student's *t* test) for $n \geq 10$ siliques are indicated by different letters. Abbreviations: α-CBD, anti-chitin binding domain antibody; α-FLAG, anti-FLAG antibody; α-HA, anti-hemagglutinin antibody; α-MBP, anti-maltose binding protein; L-W, -Leu-Trp; -L-W-H-A, -Leu-Trp-His-Ade; Nub/Cub, N/C- terminal ubiquitin.

DMPs seemed possible, as seed formation in *dmp8/9* mutant plants was not abolished but reduced to ~40% (*SI Appendix*, Fig. S1). When testing all 10 DMPs in MbY2H we found that HAP2/GCS1 also interacts with DMP3 and DMP5 but no other DMPs (Fig. 2*E*). Nevertheless, a role for DMP3 and DMP5 as HAP2/GCS1 partner proteins in sperm cells is unlikely, as *DMP3* and *DMP5* transcripts were not detected in pollen (35) and no further reduction in seed set was observed in two of independent *dmp3/5/8/9* quadruple mutant lines, generated by CRISPR/Cas9 targeted mutagenesis of *DMP3* and *DMP5* in the *dmp8/9* genomic background (*SI Appendix*, Fig. S6 *A–C*). Thus, we expressed *DMP*s by the *DMP9* promoter in *dmp8/9* sperm cells. The results showed that DMP10, which did not interact with HAP2/GCS1 in MbY2H, failed to rescue seed abortion phenotype (Fig. 2 *F–H*). DMP3, which could interact with HAP2/GCS1, also did not rescue seed abortion phenotype in *dmp8/9*. Considering there is much longer N terminus in DMP8/9 (*SI Appendix*, Fig. S6*D*), we introduced DMP9 N terminus (1–64) into DMP3 and found that DMP3^{DMP9N} could take over the function of DMP8/9 (Fig. 2 *F–H* and *SI Appendix*, Fig. S6*D*), indicating the functional importance of the N terminus for DMP9 and the functional specificity of *Arabidopsis* DMP family members as HAP2/GCS1 partner proteins in gamete fusion.

Interactions between HAP2/GCS1 and DMP9. *Arabidopsis* HAP2/GCS1 is a type-1 membrane protein of 705 amino acids, with a long extracellular domain, a single TMD, and a rather short and histidine-rich cytoplasmic tail (7, 15, 42). To identify DMP9-interacting domains of HAP2/GCS1, we introduced deletions in its ectodomain and the cytoplasmic carboxy(C)-terminus for testing binding ability. Notably, their interaction with DMP9 was not compromised when HAP2 lacked the C terminus (596–705, leaving 13 amino acids adjacent to TM domain), or when defined regions of the HAP2 ectodomain were deleted according the

HAP2 crystal structure (43) (Fig. 3*A* and *SI Appendix*, Fig. S7). Even the HAP2 variant without the ectodomain (25–530) was able to weakly interact with DMP9 in yeast (Fig. 3*A* and *SI Appendix*, Fig. S8). This suggests large interaction interfaces involving both extra- and intracellular parts of HAP2, and potentially also involving the membrane-embedded domains of HAP2. Thus, our interaction studies support a previous genetic study in *Arabidopsis* showing that the extra- and intracellular parts of HAP2 are equally important to rescue the fertility in *hap2/gcs1* mutant plants (42). Although this study did not examine the subcellular location of truncated HAP2 proteins, the molecular dissection of *C. reinhardtii* HAP2 showed that its ectodomain is required for trafficking to the cell surface, whereas the cytoplasmic region is crucial to target CrHAP2 to the minus gamete mating structure and to regulate its fusion activity (44). Currently, it remains unclear whether the HAP2 forms expressed in heterologous systems could fold into a native conformation or the unproper folding forms could be generated since large segments of HAP2 were deleted in the MbY2H assays.

Evolutionary Conservation of DMP8/9-Like Proteins as HAP2/GCS1 Partner Proteins in Seed Plants. HAP2/GCS1 orthologs have been identified in at least four out of the five eukaryotic kingdoms (45), but DMPs are specific for the green plant clade (Viridiplantae), suggesting a role in plant-specific processes (35, 37). *DMP* gene families are present in seed plant genomes and in the liverwort *Marchantia polymorpha*, whereas the unicellular green alga *C. reinhardtii* and the moss *Physcomitrella patens* have a single *DMP* (Fig. 3*B*). To explore their functional conservation as HAP2/GCS1 partner proteins, we chose DMPs from *C. reinhardtii*, *P. patens*, one gymnosperm (*Picea sitchensis*), and three angiosperm species (*Glycine max*, *Nicotiana tabacum*, *A. trichopoda*). Notably, the results from MbY2H interaction studies with *Arabidopsis* HAP2/GCS1 agreed with genetic complementation experiments (Fig. 3 *C–E*). Seed set in *dmp8/9* was fully restored by DMP8/9-like proteins from tobacco, soybean, and the extant basal angiosperm *A. trichopoda* (Fig. 3 *C–E*), providing evidence that DMP8/9-like proteins from flowering plant species can functionally replace each other as HAP2/GCS1 interactors. These results were in line with a recent report that DMP8/9-like proteins from multiple dicot crops can partially complement *dmp8/9* phenotypes (46). Furthermore, the gymnosperm DMP from *P. sitchensis* (PsDMP), clustering with *Arabidopsis* DMP3 and 5 in the phylogenetic tree of green plant DMPs (Fig. 3*B*), interacted with HAP2/GCS1 in MbY2H assays and showed a weak but significant capability to improve seed set in the *dmp8/9* mutant (Fig. 3 *C–E*), suggesting that DMP8/9-like proteins in seed plants share a conserved role as HAP2/GCS1 partner proteins.

By contrast, neither PpDMP from *P. patens* nor CrDMP from *C. reinhardtii* improved seed set in *dmp8/9*, although CrDMP showed a very weak interaction with *Arabidopsis* HAP2/GCS1 in the MbY2H assay (Fig. 3 *C–E*). A division-specific coevolution of HAP2/GCS1 and DMP interaction sites within the plant kingdom might be one explanation, supported by the recent identification of algal-specific structural features in the CrHAP2 ectodomain (47, 48). Likewise, CrDMP differs from seed plant DMPs by having a very short N terminus and an extended C terminus (*SI Appendix*, Fig. S6*D*). We inspected *CrDMP* expression in published transcriptome data from mating type *plus* and *minus* gametes of *C. reinhardtii* (49) and found it in both mating types, with highest expression values in activated *plus* gametes (37). Opposite to this, *CrHAP2* is selectively expressed in activated *minus* gametes (8, 49). A previous report, furthermore, showed that CrHAP2 is not retained on intracellular membranes but constitutively present on the cell surface of activated *C. reinhardtii minus* gametes, where it localizes to the tip of the mating structure (8). A role for CrDMP as CrHAP2 partner protein during mating of *C. reinhardtii* is therefore questionable and remains to be examined.

Three Sperm-Expressed DMP8/9-Like Proteins in Tobacco Redundantly Support Gamete Fusion. The functional equivalence of flowering plant DMPs in *Arabidopsis* sperm cells led us to confirm that gamete fusion in another angiosperm species is also supported by DMP8/9-like proteins. We identified three highly similar *DMP8/9-like* genes in *N. tabacum*, which were previously called *NtDMP1-3* (46) and here termed as *NtDMP9a-c*, to avoid misunderstanding that they were *Arabidopsis DMP1/2/3* homologs (*SI Appendix*, Fig. S9*A*). Semiquantitative RT-PCR revealed exclusive expression in male reproductive tissues (anthers), pollen, and sperm cells (Fig. 4*A*). Sperm cell specificity was confirmed by expressing NtDMP9a-GFP under the control of the *NtDMP9a* promoter (Fig. 4*B*). For functional studies in tobacco, two independent *Ntdmp9a-c* triple-mutant lines were generated by CRISPR/Cas9 gene editing (*SI Appendix*, Fig. S9*B*). Compared with 5.4± 0.7% in WT, the triple mutant lines exhibited 31.8 ± 5.1% and 30.0 ± 5.9% undeveloped seeds, respectively, indicating fertilization failure (Fig. 4 *C* and *D*). Reciprocal crosses proved that male but not female fertility is affected. The restored fertility of *Ntdmp9a-c* complemented with a Cas9-insensitive genomic fragment of *NtDMP9a* (*NtDMP9a*$g^{Cas9\text{-}ins}$) furthermore excluded the possibility of CRISPR/Cas9 off-target effects on seed set (Fig. 4*D*).

We verified that the male reproductive problems of *Ntdmp9a-c* are not due to defective pollen development, germination, or pollen tube growth (*SI Appendix*, Fig. S9 *C* and *D*) and examined the undeveloped seeds obtained from pollinating WT pistils with *Ntdmp9a-c* pollen. In tobacco, double fertilization is accomplished 2 d after pollination (DAP) (*SI Appendix*, Fig. S9 *E–J*). Whereas four-celled embryos are detectable in WT seeds 5 DAP, the undeveloped seeds derived from *Ntdmp9a-c* cross-pollination displayed unfertilized egg cells, which were eventually degenerated or collapsed (Fig. 4 *E–I*). To address whether *Ntdmp9a-c* sperm cells also fail to fertilize the central cell, we used the marker line *NtCYS8*$_{pro}$*:H2B-GFP*. This line shows nuclear-localized GFP in the two polar nuclei of the central cell, which remain unfused before fertilization. Two DAP, successful central cell fertilization is recognized by the formation of a larger triploid nucleus that results from the fusion of the two polar nuclei and the sperm cell nucleus. Subsequently, endosperm nuclei start to divide (*SI Appendix*, Fig. S9 *F–J*). In WT seeds 5 DAP, multiple GFP-fluorescent nuclei of dividing endosperm are visible(Fig. 4*J*). On the contrary, 51% undeveloped seeds derived from pollination with *Ntdmp9a-c* exhibited unfused polar nuclei indicative of unfertilized central cells. Other ovules (45.5%) displayed an enlarged nucleus indicative of central cell fertilization. Nevertheless, this nucleus did not proceed with endosperm development (Fig. 4 *K–M*). Taken together, our results provide evidence that gamete fusion in tobacco is also supported by DMP8/9-like proteins, with a stronger effect on sperm–egg fusion.

Discussion

It is evident that HAP2/GCS1 is required for gamete fusion in plant and animal species (7–14), but it remained unclear how the fusogen is regulated in time and space to prevent unintended or misdirected membrane fusion events in flowering plants (16, 50). Here we demonstrate that *Arabidopsis* HAP2/GCS1 interacts

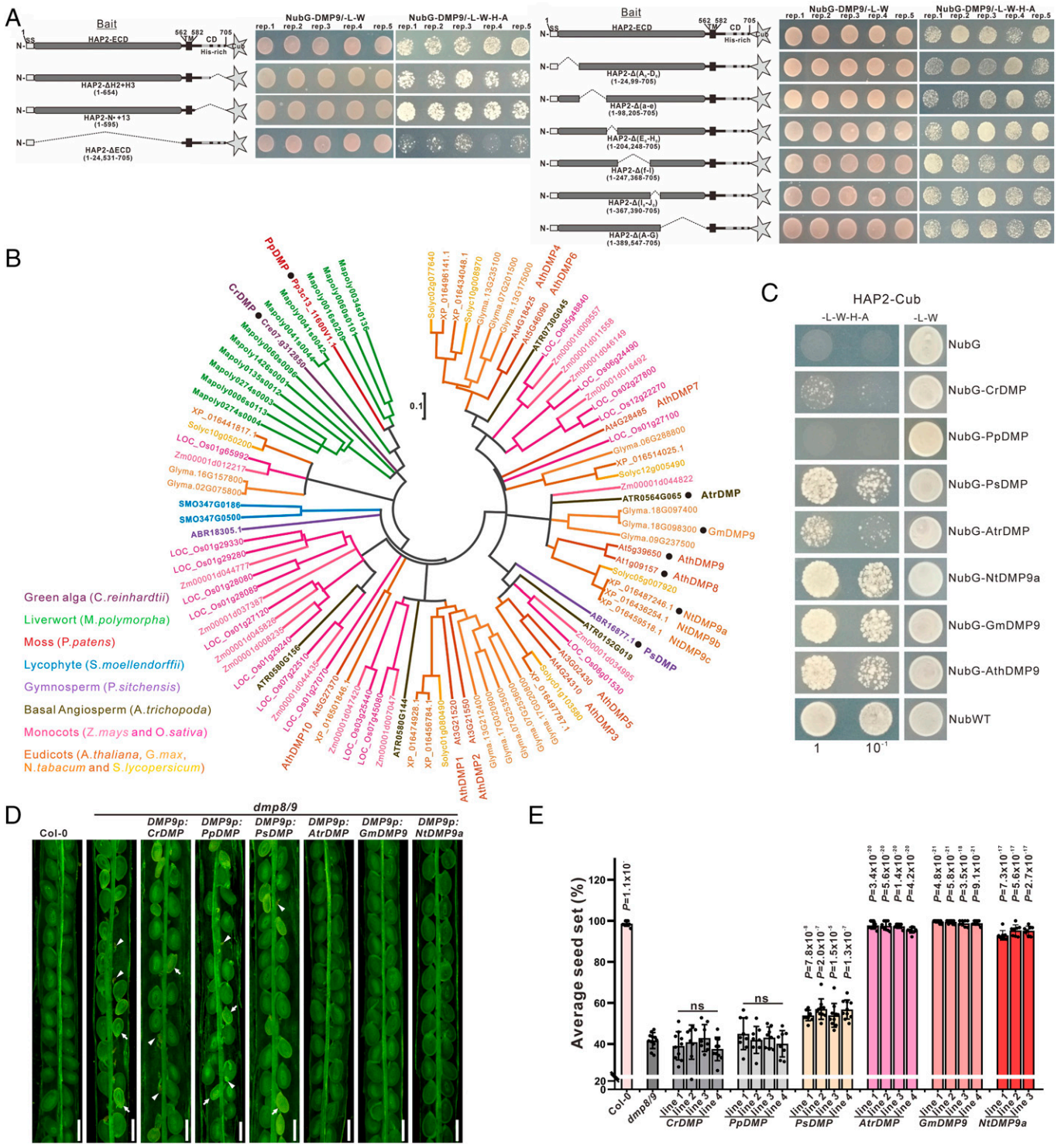

Fig. 3. Complex interactions between HAP2/GCS1 and DMP9 and functional conservation of seed plant DMP8/9-like proteins as HAP2/GCS1 partner proteins. (*A*) Membrane-based yeast-two-hybrid (MbY2H) assays to test interaction between HAP2 deletion variants fused to Cub and NubG-DMP9 (five different replicates were shown). Scheme on the left depicts the deletions within HAP2 cytoplasmic and extracellular domain, respectively. Scheme on the right depicts the defined deletions within the HAP2 extracellular domain, which are selected according the HAP2 crystal structure (42, 43). Numbers indicate terminal amino acid residues (details in *Materials and Methods*). Note that HAP2 with different deletions still interacts with *Arabidopsis* DMP9, whereas only weak interactions were observed when HAP2/GCS1 was lacking the extracellular domain. Controls for MbY2H assays are shown in *SI Appendix*, Fig. S7. (*B*) Neighbor-joining phylogenetic tree of DMPs in green plants (Viridiplantae), showing their duplication and diversification over the course of plant evolution. Black dots label those DMPs used for interaction and complementation studies. Protein IDs are listed in *SI Appendix*, Table S1. (*C*) In MbY2H assays, *Arabidopsis* HAP2/GCS1 only interacts with DMP8/9-like proteins (PsSMP, AtrDMP, NtDMP9a, GmDMP9, and AthDMP9) from seed plants. (*D*) Siliques from Col-0 (WT), *dmp8/9*, and *dmp8/9* complemented with DMP proteins from different species expressed by the *Arabidopsis DMP9* promoter. (Scale bars, 0.5 mm.) (*E*) Quantification of seed set in controls and the independent complemented lines. Data are the means ± SD of $n = 8$ to 10 siliques per line. Significant differences ($P < 0.0001$; two-sided Student's *t* test) are indicated by different letters above the columns. ns, not significant ($P > 0.05$). Abbreviations: CD, HAP2/GCS1 cytoplasmic domain; DMP9g, genomic DMP9; ECD, HAP2/GCS1 extracellular domain; His-rich, histidine-rich; SS, secretion signal; -L-W, growth medium (-Leu-Trp); -L-W-H-A, selection medium (-Leu-Trp-His-Ade); Nub/Cub, N/C-terminal ubiquitin.

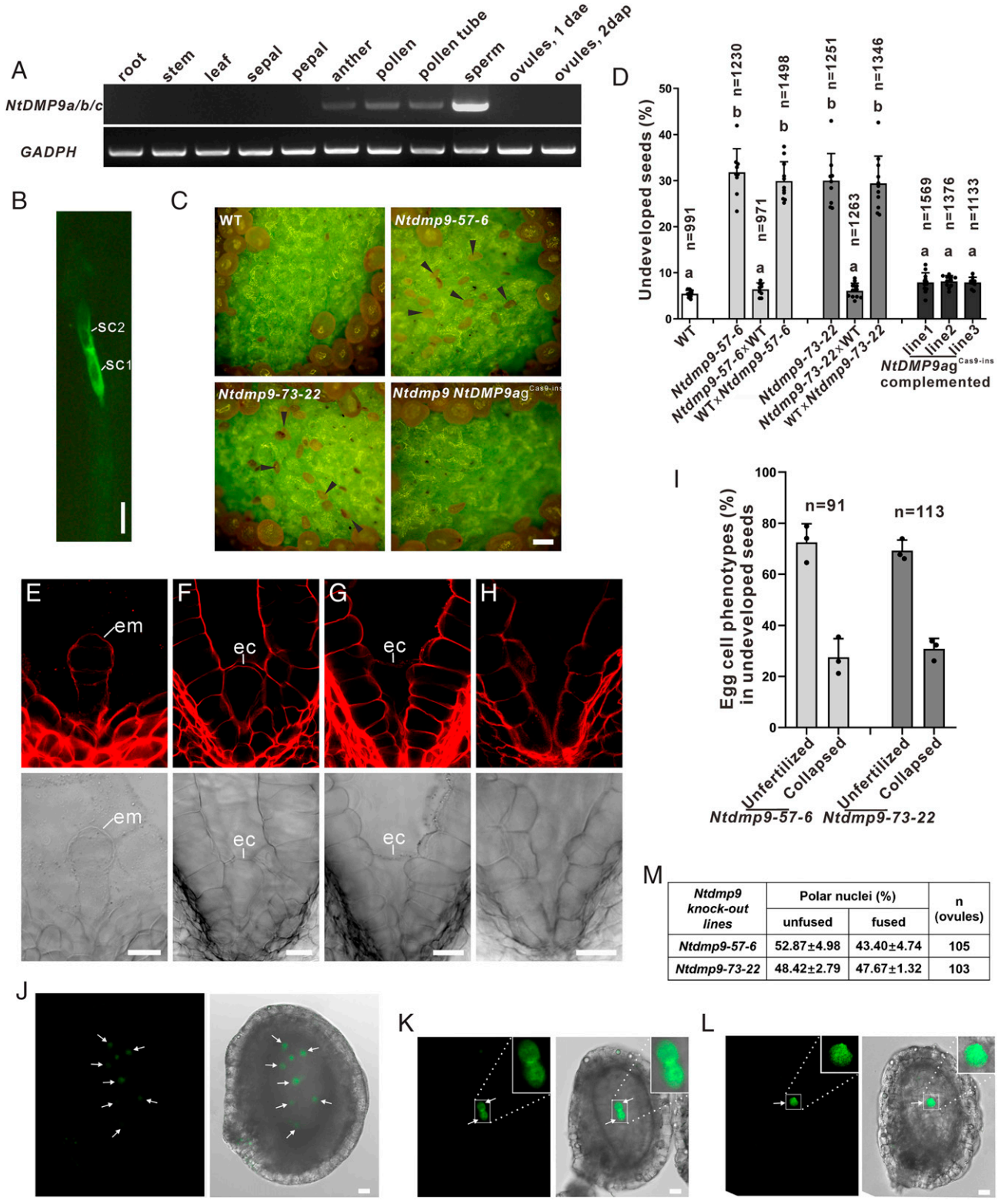

Ntdmp9 knock-out lines	Polar nuclei (%)		n (ovules)
	unfused	fused	
Ntdmp9-57-6	52.87±4.98	43.40±4.74	105
Ntdmp9-73-22	48.42±2.79	47.67±1.32	103

Fig. 4. Sperm-expressed DMP8/9-like proteins in tobacco are required for gamete fusion. (*A*) Expression of *NtDMP9a/b/c* in tobacco sperm and in bicellular pollen containing the generative cell. *GAPDH* served as control for RT-PCR. (*B*) Sperm cells expressing $NtDMP9a_{pro}$:*NtDMP9a-GFP*. (Scale bar, 10 μm.) (*C*) Tobacco ovaries 9 d after pollination (DAP). Knockout of *NtDMP9a-c* by CRISPR/Cas9 results in undeveloped seeds (arrowheads). To detect the much smaller undeveloped seeds, developing seeds were removed in the center field of view. (Scale bars, 1 mm.) (*D*) Quantification of undeveloped seeds in ovaries from WT, two *Ntdmp9a-c* lines, three complemented lines (*NtDMP9ag*$^{Cas9\text{-}ins}$ in *Ntdmp9-57-6*), and from reciprocal crosses (female × male). Data are the means ± SD. Significant differences ($P < 0.0001$ by two-sided Student's *t* test) are indicated by different letters. (*E–H*) Propidium iodide-stained seeds 5 DAP. (*E*) Micropylar region of WT seed with four-celled embryo. (*F–H*) Undeveloped ovules from pollination with *Ntdmp9a-c.* Intact egg cell (*F*), degenerating egg cell (*G*), collapsed egg cell (*H*). (Scale bars, 30 μm.) (*I*) Quantification of egg cell phenotypes. (*J–L*) Ovules expressing the central cell/endosperm marker *NtCYS8p:H2B-GFP*. (*J*) Five DAP with WT pollen. Several endosperm nuclei (arrows) are visible (>8; $n = 58$). (*K* and *L*) Undeveloped seeds 5 DAP with *Ntdmp9a-c* pollen contained either two unfused polar nuclei (*K*) or a secondary nucleus generated by fused polar nuclei (*L*). (Scale bars, 30 μm.) (*M*) Quantification of fused and unfused polar nuclei. No fluorescence was detectable in the remaining 3.73 ± 0.38% (*Ntdmp9-57-6*) and 3.91 ± 1.62% ovules (*Ntdmp9-73-22*). Data are the means ± SD. Abbreviations: dae, days after emasculation; dap, days after pollination; ec, egg cell, em, embryo; sc, sperm cell.

with sperm-expressed DMP8 and DMP9 and that these DMPs are necessary to guide HAP2/GCS1 to the sperm PM in response to a female signal. We show that this mechanism is deeply conserved in flowering plants, as all tested angiosperm DMP8/9-like proteins, including the one from most basal extant angiosperm *Amborella*, fully restored the fertility of the *Arabidopsis dmp8/9* mutant. Our studies in tobacco further proved that, also in this dicotyledonous species, gamete fusion is supported by sperm-expressed NtDMP8/9-like proteins. Thus, the evolutionary conserved molecular function of DMP8/9-like proteins in flowering plant gamete fusion offers an essential mechanism for successful fertilization.

First evidence for a timed translocation of HAP2/GCS1 to the sperm cell surface was provided in *Arabidopsis*, where HAP2/GCS1 is detected on internal membranes but redistributes to the PM when sperm cells are treated with EC1 peptides (33). We now show that *dmp8/9* sperm cells fail to translocate HAP2/GCS1 to the PM in response to EC1, demonstrating that egg cell–secreted EC1 and DMP8/9 act in the same molecular pathway. Moreover, the conjoint translocation of DMP9 and HAP2/GCS1 from membranes of discrete organelles to the cell surface and their local enrichment at the PM is indicative of an EC1-induced local formation of fusion competent sites. This process may influence sperm fusion competence specifically to the egg cell since it was previously reported that *dmp8/9* mutant sperm cell tended to fuse with the central cell (35, 38). The mechanism underlying the involvement of DMP8/9 in this interesting phenotype is worthy to be further investigated.

The timely formation of fusogenic membrane areas through the exocytic translocation of membrane proteins is remarkably reminiscent of the acrosome reaction of animal sperm (29, 51). During the acrosome reaction, part of the acrosomal membrane fuses with the PM and fertilization-relevant proteins such as mammalian IZUMO1 and SPACA6 relocate from the acrosomal membrane to the equatorial segment of the PM, which is the future site of fusion with the oolemma (30–32). Acrosome biogenesis in animal sperm remains controversial, as this organelle exhibits features of a direct Golgi derivative, a secretory granule and a lysosome-related organelle (52). Despite their morphological difference, lysosomes and vacuoles share several crucial functions, and vacuoles have previously been detected in plant sperm cells including *Arabidopsis* (53, 54). Thus, it is quite conceivable that DMP9 and HAP2/GCS1 colocalize to vacuole-related organelles before sperm activation. Upon EC1 signals from the egg cell, an acrosome-like reaction initiates the DMP9-dependent process of HAP2/GCS1 translocation from these organelles to the proper site on the sperm PM to ensure successful gamete fusion. The acrosome reaction in animal involves different proteins; therefore, whether other sperm proteins are translocated to the sperm PM by DMP8/9 and whether these proteins also contribute to the gamete fusion are very interesting questions to be answered in the near future.

Previous structural analyses showed that the ectodomain of *Arabidopsis* HAP2/GCS1 has the same three-dimensional fold as viral class II fusion proteins, which use fusion loops to insert into host cell membranes (16–18, 43). When and how the extended intermediate state of *Arabidopsis* HAP2/GCS1 is activated to inserts its fusion loop into the opposing cell membrane of a female gamete remains to be shown. Nevertheless, a constitutive enrichment of HAP2/GCS1 at the sperm cell surface might be detrimental for flowering plants, as they use a pollen tube as cellular sperm transportation system. The unique "cell within a cell" structure of pollen entails that the two nonmotile sperm cells are enclosed by an endomembrane of the pollen tube cell, which is part of the "male germ unit" involved in sperm transportation (55). The precocious exposure of HAP2/GCS1 on the sperm cell surface could therefore provoke an unintended fusion with this endomembrane, which would destroy the sperm transportation system. Despite their differences in reproductive morphology and sexual reproduction, gymnosperms also use pollen tubes for the transfer of the male gametes to the eggs (56). Although the subcellular localization and function of gymnosperm HAP2/GCS1 in male gametes remains to be explored, the discovery that a DMP from Sitka spruce interacts with *Arabidopsis* HAP2/GCS1 and partially rescues the fertilization failure in *Arabidopsis dmp8/9* suggests that seed plants utilized DMPs as HAP2/GCS1 partner proteins to accomplish HAP2/GCS1 exocytic translocation already before gymnosperms diverged from their sister plant clade of flowering plants 300 Ma.

Materials and Methods

Plant Materials and Growth Conditions. *A. thaliana* (accession Col-0) and *Nicotiana benthamiana* plants were grown in the greenhouse under a photoperiod of 16 h light and 8 h dark at 22 °C. *N. tabacum* L. cv. Petite Havana SR1 plants were grown under a 16-/8-h light/dark cycle at 25 °C. The background of all *Arabidopsis* marker lines was Col-0. Previously published marker lines used in this study were $HTR10_{pro}$*:HTR10-mRFP* (57). The T-DNA insertion lines *dmp8* (SALK_005327C) and *dmp9* (SK30238) were obtained from the Nottingham *Arabidopsis* Stock Centre.

Constructs for Plant Transformation. All primers used for cloning are listed in *SI Appendix*, Table S2. For $DMP9_{pro}$*:DMP9-GFP*, the *DMP9* promoter and gene sequence without stop codon was amplified from genomic DNA using the primer pair *DMP9-GFP-S/A* and ligated into P094 (58) upstream of GFP after SacI/HindIII digestion. To generate the DMP8 and DMP9 complementation vectors, primer pairs *DMP8-REC-S/DMP8-REC-A* and *DMP9-GFP-S/DMP9-REC-A* were used to amplify genomic *DMP8* and *DMP9*, respectively. Amplicons were digested with SacI and XhoI and cloned into P091, which was modified from pART27 (59) by inserting $LAT52_{pro}$*:GFP* to facilitate the identification of homozygous transgenic lines. For $HAP2_{pro}$*:HAP2-RFP*, the genomic fragment including the promoter region and the gene sequence without stop codon was amplified with primer pair *HAP2-RFP-S/A* and cloned via SacI/NotI restriction sites into the destination vector P182, which was modified from pART27 by adding the mRFP coding sequence.

For the *DMP3/5* CRISPR/Cas9 vector, *DMP3* and *DMP5* were each targeted by one single-guide RNA (sgRNA). The PCR fragments with two targets were amplified from pCBC-DT1T2 (60) and integrated into pENTR-MSR (61) to form two gRNA cassettes after BsaI digest. The expression cassettes were digested with KpnI/XbaI and ligated into KpnI/SpeI-digested pCAMBIA1300-pYAO-cas9 (62).

To generate the expression vectors for the complementation of *dmp8/9* with DMPs from other species, a 400-bp *DMP9* terminator fragment was amplified from genomic DNA using *REC-T-DMP9-S/A* and integrated into the destination vector P091 after AvrII and EcoRI digestion. Subsequently, the *DMP9* promoter was amplified from genomic DNA with primer pair *REC-pDMP9-S/A* and cloned into $P091\text{-}DMP9_{ter}$ after digestion by SacI and XhoI. The resulting vector $P091\text{-}DMP9_{pro}$*::*$DMP9_{ter}$ was digested with XhoI and AvrII to ligate the respective *DMP* coding sequence between the *DMP9* promoter and terminator. *DMP* coding sequences from the different plant species were amplified from genomic DNA using the REC-CDS-S/A primer pairs listed in *SI Appendix*, Table S2.

For the construct $NtDMP9a_{pro}$*:NtDMP9a-GFP*, the *NtDMP9a* promoter and gene sequence without stop codon was amplified using the primer pair *NtDMP9a-GFP-S/A* from tobacco genomic DNA and inserted into the KpnI/NotI–digested destination vector P094 (58). The *NtDMP9a/b/c* CRISPR/Cas9 vector was generated using a robust CRISPR/Cas9 vector system for targeting multiple gene sites according to the reported methods (63). To generate the Cas9-insensitive vector $NtDMP9ag^{Cas9\text{-}ins}$, the *NtDMP9* promoter was amplified with primer pair *NtDMP9a-GFP-S/NtDMP9a-REC-A-1* and ligated into KpnI/BamHI–digested pCAMBIA1300, resulting in $pCAMBIA1300\text{-}NtDMP9a_{pro}$. Two *NtDMP9a* fragments with

mutated sgRNA sites were PCR-amplified using primer pairs *NtDMP9a-REC-S-2/NtDMP9a-MUT-A* and *NtDMP9a-MUT-S/NtDMP9a-REC-A-2*, fused by overlap extension PCR (*NtDMP9a-REC-S-2/NtDMP9a-REC-A-2*), and ligated into BamHI/SalI–digested *pCAMBIA1300-NtDMP9a*$_{pro}$. *NtDMP9a* sgRNA site 1 (AGCAAAGTACTGAGGGAAT) in *NtDMP9ag*$^{Cas9\text{-}ins}$ was mutated to AACAGAGCACAGAAGGTAT; sgRNA site 2 (TGGTCCTTCCATCAGTCTA) was mutated to TGGTGCTCCCTTCCGTTTA.

All constructs were verified by sequencing and subsequently used to transform *Arabidopsis* by floral dip (64) or *N. tabacum* by *Agrobacterium*-mediated leaf disk transformation (65). Transgenic *Arabidopsis* seedlings were either selected on plates with half-strength Murashige and Skoog (MS) medium supplemented with the respective antibiotic (30 μg/mL hygromycin B or 50 μg/mL kanamycin) or by spraying 3-d-old soil-grown seedlings with BASTA (200 mg/L glufosinate ammonium, 0.1% [vol/vol] Tween-20). BASTA selection was repeated at least two times at intervals of 2 d. Transgenic *N. tabacum* seedlings were selected on MS medium containing 100 μg/mL kanamycin or 30 μg/mL hygromycin B, in addition to 250 μg/mL carbenicillin.

After selecting seedlings transgenic for a CRISPR/Cas9 T-DNA, gene editing events were analyzed by amplifying the genomic region that flanks the sgRNA target site by PCR, followed by sequencing.

For *HAP2*$_{pro}$*:HAP2-RFP* in *dmp8/9*, we crossed plants homozygous for *HAP2-RFP* (in Col-0) with *dmp8/9* and screened for double-homozygous *HAP2-RFP dmp8/9* plants in the T3 progeny.

Phenotypic Analysis. To investigate *Arabidopsis* pollen development, the HTR10-RFP marker line was crossed into the double *dmp8/9* mutant and observed under a Leica SP8 confocal laser scanning microscope (CLSM). For in vitro pollen germination assays, mature pollen grains were spread on solid pollen germination medium (0.05% boric acid, 5 mM $CaCl_2$, 5 mM KCl, 1 mM $MgSO_4$, 10% sucrose, pH 7.5, 1% agarose) and cultured for 10 h at 22 °C. For the pollen-tube guidance, hand-pollinated pistils were fixed with ethanol:acetic acid (3:1) overnight, washed with 0.1 M phosphate-buffered saline (PBS) three times, and treated with 5 M NaOH overnight to allow softening. Then, the pistils were washed with 0.1 M PBS three times and stained with 0.1% (wt/vol) aniline blue solution containing 108 mM K_3PO4 at pH 11 and 2% glycerol. For embryo observation, the ovules were first dissected out with a fine needle and then cleared according to previously reported methods (66).

Tobacco pollen was germinated in liquid germination medium [5 μM $CaCl_2$, 5 μM $Ca(NO3)_2$, 1 mM $Mg(SO4)_2$, 0.01% H_3BO_3, and 18% sucrose, pH 6.8]. For DAPI (4,6-diamidino-2-phenylindole) staining, pollen tubes were incubated in a liquid germination medium containing 2.5 μg/mL DAPI and 0.01% (vol/vol) Triton X-100 in the dark for 10 min before imaging by fluorescence microscopy. For tobacco seed clearing, the collected seeds were first fixed with 10% acetic acid in 50% methanol (4 °C, 12 h), followed by an overnight treatment in 0.2 M NaOH with 1% sodium dodecyl sulfate (SDS) at room temperature. Thereafter, the seeds were washed in water then incubated in 2.5% NaClO for 1 h. Subsequently, the seeds were rinsed again and incubated in 1% periodic acid for 1 h at room temperature, followed by 80% ethanol for 10 min at 80 °C. Then the seeds were transferred back to the fixative (10% acetic acid in 50% methanol) for 1 h and rinsed again with water. Afterward, the samples were stained by Schiff reagent with propidium iodide (P4170; Sigma) (100 mM sodium metabisulphite and 0.15 M HCl; propidium iodide to a final concentration of 0.1 mg/mL) for about 6 to 24 h and transferred to a chloral hydrate solution (4 g chloral hydrate, 1 mL glycerol, and 2 mL water) for overnight incubation at room temperature. Finally, the seeds were cleared at least for 10 d in Hoyer's solution (30 g gum arabic, 200 g chloral hydrate, 20 g glycerol, and 50 mL water) before they were observed under a confocal microscope (Leica SP8 CLSM). The excitation wavelength was 552 nm, and the emission wavelengths were 562 to 660 nm.

Sperm Activation Assays and Immunofluorescence. Sperm cell activation assays were performed as previously described (33). Two high-performance liquid chromatography–purified peptides covering the EC1.1 signature motifs S1 (CSGELILFFLNGETYIGPG) and S2 (CWPTMIGVLGFTAQEGDMLQGY) were synthesized by GenScript. Peptides were diluted as described (33), with a final peptide concentration 120 μM each and 2% dimethyl sulfoxide (DMSO) in liquid pollen germination medium. The peptide-free control solution was 2% DMSO in liquid pollen germination medium. In Fig. 1*D*, we assessed the sperm cells for the presence of a continuous HAP2-YFP signal along the sperm PM in four independent experiments. In Fig. 1*G*, we first assessed whether HAP2/GCS1-RFP colocalized with DMP9-GFP in vesicle-like bodies and then counted the percentage of sperm cells with colocalized vesicles, which were at PM areas or only intracellular, respectively. For immunofluorescent labeling of HAP2/GCS1, when pollen tubes emerged from the style they were immediately cut off and fixed in 1% formaldehyde containing 0.1% Triton X-100 for 40 min with gentle rotation. After three washes with TTBS buffer (Tris-buffered saline [TBS] buffer with 0.1% Triton X-100), samples were incubated in TBS containing 10% DMSO (D2650; Sigma-Aldrich) and 3% Nonidet P-40 (M158; Amresco) for 1 h to enhance permeability. Samples were washed and incubated in blocking buffer (TBS, 0.1%Triton X-100, 5% BSA) for 1 h. Then, samples were incubated with primary antibodies (TagRFP Polyclonal Antibody, R10367, 1:100; Invitrogen) for 24 h at 4 °C and washed three times for 1 h each. Finally, samples were incubated with anti-rabbit Alexa Fluor 488 (A-11006, 1:1,000; Invitrogen) for 24 h at 4 °C and washed twice in 1 TTBS for 1 h each time.

Semiquantitative RT-PCR. For semiquantitative PCR in tobacco, different samples from *N. tabacum* L. cv. Petite Havana SR1 were collected for total RNA isolation using TaKaRa MiniBEST Plant RNA Extraction Kit. First-strand complementary DNA synthesis was performed using MLV-reverse transcriptase following the manufacturer's instructions (Invitrogen). *GADPH* was used as the reference gene. All primer pairs used for analyzing gene expression are listed in *SI Appendix*, Table S2.

Phylogenetic Analysis and TMD Prediction. PLAZA (https://bioinformatics.psb.ugent.be/plaza/), Phytome(https://phytozome-next.jgi.doe.gov/), and NCBI (https://www.ncbi.nlm.nih.gov/) were used to search for DMP proteins in different plant species, based on the 10 *Arabidopsis* DMPs reported by Kasaras and Kunze (41). For phylogenetic analyses, DUF679-containing protein family members from a green alga (*C. reinhardtii*), a liverwort (*M. polymorpha*), a bryophyte (*P. patens*), a lycophyte (*Selaginella moellendorffii*), a gymnosperm (*P. sitchensis*), a basal angiosperm (*A. trichopoda*), two monocots (*Zea mays*, *Oryza sativa*), and four eudicots (*A. thaliana*, *G. max*, *N. tabacum*, and *Solanum lycopersicum*) were included. Protein IDs are listed in *SI Appendix*, Table S1. One DMP sequence of *P. patens* (Pp3c13_21560V1.1) was too short and therefore not included in the phylogenetic tree. Multiple sequence alignment of DMP proteins was performed using Clustal X v2.1 with the default multiple alignment parameters. The phylogenetic tree was constructed with MEGA5 using the neighbor-joining method. The tree is drawn to scale, with branch lengths in the same units as those of the evolutionary distances used to infer the phylogenetic tree. The evolutionary distances were computed using the Poisson correction method and are in the units of the number of amino acid substitutions per site.

TMD predictions for different DMPs were assigned according to Deep TMHMM (67) and the scheme depicting the transmembrane topology of DMP9 in Fig. 2*F* was prepared by Protter (wlab.ethz.ch/protter/start/) using transmembrane regions annotated by UniProt, with the N-terminal location intracellular (68, 69).

DUAL Membrane Yeast-Two-Hybrid Assays. Membrane-based split-ubiquitin yeast-two-hybrid assays were performed according to the DUALmembrane starter kit manual (Dualsystems Biotech). In brief, yeast strain NMY51 was cotransformed with a bait and prey vector by the lithium acetate transformation method for 48 h, and protein–protein interactions were scored based on growth on SD medium lacking leucine, tryptophane, adenine, and histidine (-L-W-H-A). *Arabidopsis* HAP2 and HAP2 deletions were cloned in the prey vector pBT3-C. DMPs from *Arabidopsis, Chlamydomonas*, and other plant species were cloned in the bait vector pPR3-N. A functional HAP2 variant lacking the histidine-rich H2 and H3 domains at the C terminus (HAP2-ΔH2+H3) (42) was amplified with primer pair *HAP2-Cub-S*/*HAP2-Cub–ΔH2+H3-A-1*. A nonfunctional HAP2 variant lacking the whole cytoplasmic domain similar to AtN● +13 (42) was amplified with primer pair *HAP2-Cub-S*/*HAP2-Cub–ΔC-A-1*. To generate HAP2-ΔECD, primer pairs *HAP2-Cub-S*/*HAP2-Cub–ΔN-A-1* and *HAP2-Cub–ΔN-S-1*/*HAP2-Cub-A* were used. For different deletions within the extracellular domain, two HAP2 fragments were PCR-amplified using *HAP2-Cub-S*/*HAP2-Cub–Δ-A-1* and *HAP2-Cub–Δ-S-1*/*HAP2-Cub-A*, fused by overlap extension PCR (*HAP2-Cub-S*/*HAP2-Cub-A*) and ligated into pBT3-C using SfiI. Deleted domains were selected according the HAP2 crystal structure (43). Δ(A_0-D_0) is a deletion of amino acids

25 to 98, Δ(a-e) is a deletion of amino acids 99 to 204, Δ(E_0-H_0) is a deletion of amino acids 205 to 247, Δ(f-l) is a deletion of amino acids 248 to 367, Δ(I_0-J_0) is a deletion of amino acids 368 to 389, and Δ(A-G) is a deletion of amino acids 390 to 546. All primers used to generate the different deletions are listed in *SI Appendix*, Table S2.

Recombinant His-MBP Protein Expression and Purification. For the His-MBP control protein, 6xHis-MBP was amplified from pMAL-c2X (New England Biolabs, Inc.) using the primer pair *HIS-MBP-pET30a-S/A* and cloned into pET30a (Novagen). The 6xHis-MBP expression vector was transformed into *Escherichia coli* BL21 (DE3) and His-MBP was expressed and purified according to the manufacturer's instructions.

Pull-Down Assays. To express the MBP-$HAP2_{ecd}$ fusion protein in *E. coli*, the extracellular domain of HAP2 lacking the putative signal sequence was amplified with the primer pair *HAP2-N-MBP-S/A* and cloned into EcoRI/XbaI–digested expression vector pMAL-c2X (New England Biolabs). To express DMP-intein fusion proteins, the MBP sequence in the control plasmid pMXB10 (NEB no. N6903) was removed by NdeI and XhoI digestion and replaced either by the DMP8 or DMP9 coding sequence, amplified with primer pairs *DMP8-intein-S/A* and *DMP9-intein-S/A*, respectively. To express 6xHis-DMP-intein fusion proteins, primer pairs *HIS-DMP8-intein-S/DMP8-intein-A* and *HIS-DMP9-intein-S/DMP9-intein-A* were used.

Expression vectors were transformed into *E. coli* BL21 (DE3). The recombinant MBP-$HAP2_{ecd}$, DMP-Intein and His-DMP-Intein were expressed in the cytoplasm. Procedures for the expression of recombinant MBP- and Intein-fusion proteins in *E. coli* and the extraction of crude protein were according to the manufacturer's instructions. Induction of protein expression was at 15 °C for 24 h with 0.4 mM isopropyl β-D-1-thiogalactopyranoside (optical density at 600 nm = 0.6). TBS (20 mM Tris-HCl, pH 7.2, 200 mM NaCl, 1 mM ethylenediaminetetraacetic acid [EDTA]) plus 1× protease inhibitor mixture (Roche) and 0.5% Triton X-100 was used as lysis buffer. For MBP pull-down assays, the amylose resin (New England Biolabs) was washed three times with TBS buffer. MBP-HAP2/$GCS1_{ecd}$ and MBP protein in bacterial lysates was bound to 50 μL amylose resin by incubation for 1 h at 4 °C. The supernatants were discarded and the amylose resins were washed five times with TBS buffer (plus 0.1% Triton X-100). The crude protein extract for Intein-fusion proteins was added to the amylose resin and incubated for 2 h at 4 °C with gentle rocking. The supernatant was discarded and the resin was washed at least five times with 1 mL TBS buffer (plus 0.1% Triton X-100) each time. Bound proteins were eluted in 1× SDS sample buffer by heating at 95 °C for 5 min. Proteins were separated in sodium dodecyl sulfate polyacrylamide gel electrophoresis (SDS-PAGE) (12%), blotted onto poly(vinylidene difluoride) (PVDF) membranes, and immunostained with monoclonal anti-MBP or anti-CBD (New England Biolabs) as primary and peroxidase-labeled goat anti-mouse immunoglobulin G (IgG) as secondary antibody (ABclonal). Immun-Star HRP Chemiluminescent Substrate (Bio-Rad) was used for detection. All the experiments were repeated three times.

Coimmunoprecipitation (Co-IP) experiments. *$35S_{pro}$:3×HA* and *$35S_{pro}$:3×Flag* cloning vectors were created by inserting the fragment *$35S_{pro}$:3×HA-Nos_{ter}* or *$35S_{pro}$:3×Flag-Nos_{ter}* into pART27 (59). To generate *$35S_{pro}$:DMP8-3×HA* and *$35S_{pro}$:DMP9-3×HA* expression vectors, *DMP8* and *DMP9* coding sequences were amplified from genomic DNA using primer pairs *35S-DMP8-HA-S/A* and *35S-DMP9-HA-S/A*, respectively, and cloned into *$35S_{pro}$:3×HA* after XbaI/EcoRI digestion. For *$35S_{pro}$:HAP2-N-3×Flag*, the extracellular domain of HAP2 lacking the putative signal sequence was amplified from the vector *HAP2-N-pMAL-c2X* with the primer pair *35S-HAP2-N-FLAG-S/A* and integrated into *$35S_{pro}$:3×Flag* after XbaI/EcoRI digestion. Expression vectors were transformed into *Agrobacterium tumefaciens* GV3101 followed by *N. benthamiana* leaf infiltration as described previously (70). Hemagglutinin (HA) IPs were performed according to the Anti-HA Immunoprecipitation Kit (IP0010; Sigma) with small modification. After 48 h, infiltrated leaves were collected, ground in liquid nitrogen, and resuspended in cold CelLytic M Cell Lysis buffer (C2978) plus 1× protease inhibitor mixture. The crude protein extract was centrifuged three times for 15 min at 16,000 × *g* at 4 °C before the supernatant was added to 10 μL anti-HA Agarose, which was preequilibrated by washing three times with self-prepared co-IP buffer (15 mM Tris-HCl, pH 7.5, 150 mM NaCl, 1 mM EDTA). After incubation on an orbital shaker at 4 °C for 2 h, the anti-HA Agarose was washed seven times with each 700 μL IP buffer (diluted from 10× IP Buffer, catalog no. I5779). Immunoprecipitates were eluted in 1× SDS sample buffer (50 μL) by heating at 95 °C for 5 min. The protein samples were separated by SDS-PAGE (10%), blotted onto PVDF membrane, and stained with polyclonal anti-HA or anti-Flag as primary and peroxidase-labeled goat anti-rabbit or mouse IgG as secondary antibody (ABclonal). Immun-Star HRP Chemiluminescent Substrate (Bio-Rad) was used for detection. As for Flag IPs, the lysis buffer was self-prepared Co-IP buffer (plus 1% Triton X-100 and 1× protease inhibitor mixture) and anti-Flag Affinity Gelfrom Bimake (B23101) were used and washed with self-prepared Co-IP buffer plus 0.1% Triton X-100. All the experiments were repeated three times.

For EC1.1 and DMP9 co-IP experiments, DMP9-3xHA was transiently expressed in *N. benthamiana* and the crude protein extract was prepared as HA IPs; 0.5 μg recombinant His-MBP-EC1.1 or His-MBP control protein was added to 600 μL tobacco protein supernatant with Anti–HA-Agarose and incubated for 2 h on an orbital shaker at 4 °C. EC1.1 and DMP9 co-IP experiments were performed as described above, with polyclonal anti-HA or anti-His (ABclonal) as primary antibodies for immunostaining. This experiment was repeated six times.

Quantification and Statistical Analysis. Statistical significance was determined using Student's *t* test and calculated using GraphPad Prism software (GraphPad Software) or T.TEST in Excel. The error bars, statistical methods, and *n* values for all experiments are indicated in figures or figure legends. Each experiment was repeated independently at least three times with similar results, unless otherwise stated. Figures were prepared using Adobe Photoshop, CorelDRAW, or PowerPoint.

Data, Materials, and Software Availability. All study data are included in the article and/or supporting information.

ACKNOWLEDGMENTS. We are grateful to Stefanie Sprunck (University of Regensburg) for providing *5xec1* seeds and HIS-MBP-EC1.1 protein and also for critical comments on the manuscript. We thank Y. G. Liu (South China Agricultural University) for providing the CRISPR/Cas9 system used in tobacco and Q. J. Chen (China Agricultural University) and Q. Xie (University of Chinese Academy of Sciences) for CRISPR/Cas9 vectors used in *Arabidopsis*. We thank F. Berger (Gregor Mendel Institute of Molecular Plant Biology, Vienna, Austria) and G. Drews (University of Utah, Salt Lake City, UT) for providing marker lines, K. Huang (Chinese Academy of Sciences) for providing *C. reinhardtii* genomic DNA, and the Nottingham Arabidopsis Stock Centre for providing T-DNA insertion lines. This work was supported by National Natural Science Foundation of China grants 31991201, 32130031, and 31800264.

1. N. G. Brukman, B. Uygur, B. Podbilewicz, L. V. Chernomordik, How cells fuse. *J. Cell Biol.* **218**, 1436–1451 (2019).
2. J. M. Hernández, B. Podbilewicz, The hallmarks of cell-cell fusion. *Development* **144**, 4481–4495 (2017).
3. E. Bianchi, G. J. Wright, Find and fuse: Unsolved mysteries in sperm-egg recognition. *PLoS Biol.* **18**, e3000953 (2020).
4. R. W. Doms, What came first-the virus or the egg? *Cell* **168**, 755–757 (2017).
5. W. J. Snell, Uncovering an ancestral green *ménage à trois*: Contributions of *Chlamydomonas* to the discovery of a broadly conserved triad of plant fertilization proteins. *Curr. Opin. Plant Biol.* **69**, 102275 (2022).
6. S. Sprunck, Twice the fun, double the trouble: Gamete interactions in flowering plants. *Curr. Opin. Plant Biol.* **53**, 106–116 (2020).
7. T. Mori, H. Kuroiwa, T. Higashiyama, T. Kuroiwa, GENERATIVE CELL SPECIFIC 1 is essential for angiosperm fertilization. *Nat. Cell Biol.* **8**, 64–71 (2006).
8. Y. Liu *et al.*, The conserved plant sterility gene *HAP2* functions after attachment of fusogenic membranes in Chlamydomonas and Plasmodium gametes. *Genes Dev.* **22**, 1051–1068 (2008).
9. M. Hirai *et al.*, Male fertility of malaria parasites is determined by GCS1, a plant-type reproduction factor. *Curr. Biol.* **18**, 607–613 (2008).
10. E. S. Cole *et al.*, Function of the male-gamete-specific fusion protein HAP2 in a seven-sexed ciliate. *Curr. Biol.* **24**, 2168–2173 (2014).
11. H. Kawai-Toyooka *et al.*, Sex-specific posttranslational regulation of the gamete fusogen GCS1 in the isogamous volvocine alga *Gonium pectorale*. *Eukaryot. Cell* **13**, 648–656 (2014).
12. E. Ebchuqin *et al.*, Evidence for participation of GCS1 in fertilization of the starlet sea anemone *Nematostella vectensis*: Implication of a common mechanism of sperm-egg fusion in plants and animals. *Biochem. Biophys. Res. Commun.* **451**, 522–528 (2014).
13. M. Okamoto *et al.*, Two HAP2-GCS1 homologs responsible for gamete interactions in the cellular slime mold with multiple mating types: Implication for common mechanisms of sexual reproduction shared by plants and protozoa and for male-female differentiation. *Dev. Biol.* **415**, 6–13 (2016).
14. M. Camacho-Nuez *et al.*, *Hap2*, a novel gene in *Babesia bigemina* is expressed in tick stages, and specific antibodies block zygote formation. *Parasit. Vectors* **10**, 568 (2017).

15. K. von Besser, A. C. Frank, M. A. Johnson, D. Preuss, *Arabidopsis* HAP2 (GCS1) is a sperm-specific gene required for pollen tube guidance and fertilization. *Development* **133**, 4761–4769 (2006).
16. J. Fédry *et al.*, The ancient gamete fusogen HAP2 is a eukaryotic class II fusion protein. *Cell* **168**, 904–915.e10 (2017).
17. J. F. Pinello *et al.*, Structure-function studies link class II viral fusogens with the ancestral gamete fusion protein HAP2. *Curr. Biol.* **27**, 651–660 (2017).
18. C. Valansi *et al.*, *Arabidopsis* HAP2/GCS1 is a gamete fusion protein homologous to somatic and viral fusogens. *J. Cell Biol.* **216**, 571–581 (2017).
19. S. C. Harrison, Viral membrane fusion. *Virology* **479-480**, 498–507 (2015).
20. M. Kielian, F. A. Rey, Virus membrane-fusion proteins: More than one way to make a hairpin. *Nat. Rev. Microbiol.* **4**, 67–76 (2006).
21. Y. Modis, I. I. Class, Class II fusion proteins. *Adv. Exp. Med. Biol.* **790**, 150–166 (2013).
22. J. Zhang *et al.*, Species-specific gamete recognition initiates fusion-driving trimer formation by conserved fusogen HAP2. *Nat. Commun.* **12**, 4380 (2021).
23. J. F. Pinello, Y. Liu, W. J. Snell, MAR1 links membrane adhesion to membrane merger during cell-cell fusion in *Chlamydomonas*. *Dev. Cell* **56**, 3380–3392.e9 (2021).
24. P. J. Ferris, J. P. Woessner, U. W. Goodenough, A sex recognition glycoprotein is encoded by the plus mating-type gene *fus1* of *Chlamydomonas reinhardtii*. *Mol. Biol. Cell* **7**, 1235–1248 (1996).
25. M. J. Misamore, S. Gupta, W. J. Snell, The *Chlamydomonas* Fus1 protein is present on the mating type plus fusion organelle and required for a critical membrane adhesion event during fusion with minus gametes. *Mol. Biol. Cell* **14**, 2530–2542 (2003).
26. T. Mori, T. Igawa, G. Tamiya, S. Y. Miyagishima, F. Berger, Gamete attachment requires GEX2 for successful fertilization in *Arabidopsis*. *Curr. Biol.* **24**, 170–175 (2014).
27. E. Bianchi, G. J. Wright, Sperm meets egg: The genetics of mammalian fertilization. *Annu. Rev. Genet.* **50**, 93–111 (2016).
28. A. R. Krauchunas, M. R. Marcello, A. Singson, The molecular complexity of fertilization: Introducing the concept of a fertilization synapse. *Mol. Reprod. Dev.* **83**, 376–386 (2016).
29. N. Hirohashi, R. Yanagimachi, Sperm acrosome reaction: Its site and role in fertilization. *Biol. Reprod.* **99**, 127–133 (2018).
30. S. Barbaux *et al.*, Sperm SPACA6 protein is required for mammalian sperm-egg adhesion/fusion. *Sci. Rep.* **10**, 5335 (2020).
31. T. Noda *et al.*, Sperm proteins SOF1, TMEM95, and SPACA6 are required for sperm-oocyte fusion in mice. *Proc. Natl. Acad. Sci. U.S.A.* **117**, 11493–11502 (2020).
32. Y. Satouh, N. Inoue, M. Ikawa, M. Okabe, Visualization of the moment of mouse sperm-egg fusion and dynamic localization of IZUMO1. *J. Cell Sci.* **125**, 4985–4990 (2012).
33. S. Sprunck *et al.*, Egg cell-secreted EC1 triggers sperm cell activation during double fertilization. *Science* **338**, 1093–1097 (2012).
34. S. Rademacher, S. Sprunck, Downregulation of egg cell-secreted EC1 is accompanied with delayed gamete fusion and polytubey. *Plant Signal. Behav.* **8**, e27377 (2013).
35. P. Cyprys, M. Lindemeier, S. Sprunck, Gamete fusion is facilitated by two sperm cell-expressed DUF679 membrane proteins. *Nat. Plants* **5**, 253–257 (2019).
36. T. Dresselhaus, S. Sprunck, G. M. Wessel, Fertilization mechanisms in flowering plants. *Curr. Biol.* **26**, R125–R139 (2016).
37. T. Takahashi *et al.*, The male gamete membrane protein DMP9/DAU2 is required for double fertilization in flowering plants. *Development* **145**, dev170076 (2018).
38. H. Xiong, W. Wang, M. X. Sun, Endosperm development is an autonomously programmed process independent of embryogenesis. *Plant Cell* **33**, 1151–1160 (2021).
39. Y. Zhong *et al.*, A DMP-triggered in vivo maternal haploid induction system in the dicotyledonous *Arabidopsis*. *Nat. Plants* **6**, 466–472 (2020).
40. Y. Hamamura *et al.*, Live-cell imaging reveals the dynamics of two sperm cells during double fertilization in *Arabidopsis thaliana*. *Curr. Biol.* **21**, 497–502 (2011).
41. A. Kasaras, R. Kunze, Expression, localisation and phylogeny of a novel family of plant-specific membrane proteins. *Plant Biol.* **12** (suppl. 1), 140–152 (2010).
42. J. L. Wong, A. R. Leydon, M. A. Johnson, HAP2(GCS1)-dependent gamete fusion requires a positively charged carboxy-terminal domain. *PLoS Genet.* **6**, e1000882 (2010).
43. J. Fedry *et al.*, Evolutionary diversification of the HAP2 membrane insertion motifs to drive gamete fusion across eukaryotes. *PLoS Biol.* **16**, e2006357 (2018).
44. Y. Liu, J. Pei, N. Grishin, W. J. Snell, The cytoplasmic domain of the gamete membrane fusion protein HAP2 targets the protein to the fusion site in *Chlamydomonas* and regulates the fusion reaction. *Development* **142**, 962–971 (2015).
45. J. L. Wong, M. A. Johnson, Is HAP2-GCS1 an ancestral gamete fusogen? *Trends Cell Biol.* **20**, 134–141 (2010).
46. Y. Zhong *et al.*, Establishment of a *dmp* based maternal haploid induction system for polyploid *Brassica napus* and *Nicotiana tabacum*. *J. Integr. Plant Biol.* **64**, 1281–1294 (2022).
47. E. Baquero, J. Fedry, P. Legrand, T. Krey, F. A. Rey, Species-specific functional regions of the green alga gamete fusion protein HAP2 revealed by structural studies. *Structure* **27**, 113–124.e4 (2019).
48. J. Feng *et al.*, Fusion surface structure, function, and dynamics of gamete fusogen HAP2. *eLife* **7**, ●●● (2018).
49. J. Ning *et al.*, Comparative genomics in *Chlamydomonas* and *Plasmodium* identifies an ancient nuclear envelope protein family essential for sexual reproduction in protists, fungi, plants, and vertebrates. *Genes Dev.* **27**, 1198–1215 (2013).
50. T. Clark, HAP2/GCS1: Mounting evidence of our true biological EVE? *PLoS Biol.* **16**, e3000007 (2018).
51. R. Yanagimachi, Mammalian sperm acrosome reaction: Where does it begin before fertilization? *Biol. Reprod.* **85**, 4–5 (2011).
52. M. B. Khawar, H. Gao, W. Li, Mechanism of acrosome biogenesis in mammals. *Front. Cell Dev. Biol.* **7**, 195 (2019).
53. M. Weber, Formation of sperm cells in *Galium-mollugo* (Rubiaceae), *Trichodiadema-setuliferum* (Aizoaceae), and *Avena-sativa* (Poaceae). *Plant Syst. Evol.* **161**, 53–64 (1988).
54. M. M. Wudick, D. T. Luu, C. Tournaire-Roux, W. Sakamoto, C. Maurel, Vegetative and sperm cell-specific aquaporins of *Arabidopsis* highlight the vacuolar equipment of pollen and contribute to plant reproduction. *Plant Physiol.* **164**, 1697–1706 (2014).
55. A. D. McCue, M. Cresti, J. A. Feijó, R. K. Slotkin, Cytoplasmic connection of sperm cells to the pollen vegetative cell nucleus: Potential roles of the male germ unit revisited. *J. Exp. Bot.* **62**, 1621–1631 (2011).
56. J. Lora, J. I. Hormaza, M. Herrero, The diversity of the pollen tube pathway in plants: Toward an increasing control by the sporophyte. *Front Plant Sci* **7**, 107 (2016).
57. M. Ingouff, Y. Hamamura, M. Gourgues, T. Higashiyama, F. Berger, Distinct dynamics of HISTONE3 variants between the two fertilization products in plants. *Curr. Biol.* **17**, 1032–1037 (2007).
58. J. J. Wu *et al.*, Mitochondrial GCD1 dysfunction reveals reciprocal cell-to-cell signaling during the maturation of *Arabidopsis* female gametes. *Dev. Cell* **23**, 1043–1058 (2012).
59. A. P. Gleave, A versatile binary vector system with a T-DNA organisational structure conducive to efficient integration of cloned DNA into the plant genome. *Plant Mol. Biol.* **20**, 1203–1207 (1992).
60. H. L. Xing *et al.*, A CRISPR/Cas9 toolkit for multiplex genome editing in plants. *BMC Plant Biol.* **14**, 327 (2014).
61. Z. Ge *et al.*, *Arabidopsis* pollen tube integrity and sperm release are regulated by RALF-mediated signaling. *Science* **358**, 1596–1600 (2017).
62. L. Yan *et al.*, High-efficiency genome editing in *Arabidopsis* using YAO promoter-driven CRISPR/Cas9 system. *Mol. Plant* **8**, 1820–1823 (2015).
63. X. Ma *et al.*, A robust CRISPR/Cas9 system for convenient, high-efficiency multiplex genome editing in monocot and dicot plants. *Mol. Plant* **8**, 1274–1284 (2015).
64. S. J. Clough, A. F. Bent, Floral dip: A simplified method for *Agrobacterium*-mediated transformation of *Arabidopsis thaliana*. *Plant J.* **16**, 735–743 (1998).
65. R. B. Horsch *et al.*, A simple and general method for transferring genes into plants. *Science* **227**, 1229–1231 (1985).
66. H. J. Li *et al.*, POD1 regulates pollen tube guidance in response to micropylar female signaling and acts in early embryo patterning in *Arabidopsis*. *Plant Cell* **23**, 3288–3302 (2011).
67. J. Hallgren *et al.*, DeepTMHMM predicts alpha and beta transmembrane proteins using deep neural networks. *bioRxiv*, 2022.04.08.487609 (2022).
68. U. Omasits, C. H. Ahrens, S. Müller, B. Wollscheid, Protter: Interactive protein feature visualization and integration with experimental proteomic data. *Bioinformatics* **30**, 884–886 (2014).
69. A. Bateman *et al.*; UniProt Consortium, UniProt: The universal protein knowledgebase in 2021. *Nucleic Acids Res.* **49**, D480–D489 (2021).
70. N. Ohad, S. Yalovsky, Utilizing bimolecular fluorescence complementation (BiFC) to assay protein-protein interaction in plants. *Methods Mol. Biol.* **655**, 347–358 (2010).